From the Proceedings of the International Symposium on Earthquake Engineering
Commemorating the Tenth Anniversary of the 1995 Kobe Earthquake
(held on January 13-16, 2005 in Kobe/Awaji, Japan)

INTENSITY MEASURES OF GROUND MOTION FROM THE VIEWPOINT OF STRUCTURAL RESPONSES OF SMRF BUILDINGS

Yasuhiro Mori[1], Takashi Yamanaka[1], Nicolas Luco[2], and C. Allin Cornell[3]

[1] *Graduate School of Environmental Studies, Nagoya University, Japan*
E-mail: yasu@sharaku.nuac.nagoya-u.ac.jp
[2] *U.S. Geological Survey, Golden, CO, USA*
Email: nluco@usgs.gov
[3] *Department of Civil and Environmental Engineering, Stanford University, USA*

SUMMARY

The intensity of a ground motion is often measured by its maximum value, such as peak acceleration or velocity. However, from the viewpoint of structural performance evaluation and design, an intensity measure (IM) that is related more directly to structural responses and, accordingly, to structural damage, is more desirable. Luco and Cornell proposed a simple IM extending the idea of modal superposition of the first two modes with the square-root-of-sum-of-squares (SRSS) rule and taking a first-mode inelastic spectral displacement into account. This IM achieved a marked improvement over simply using the response of an elastic oscillator; however, as a "predictor" of structural response, it does not capture well large displacements caused by local yielding. A possible extension of Luco's IM is discussed in this paper that considers a post-elastic mode shape.

1. INTRODUCTION

The intensity of a ground motion is often measured by its maximum value, such as peak acceleration or velocity. However, from the viewpoint of structural performance evaluation and design, an intensity measure that is related more directly to structural responses and, accordingly, to structural damage, is more desirable. For example, the spectral acceleration of an elastic oscillator is often considered as an intensity measure. As a "predictor" (or estimate) of seismic demands, however, it does not take into account the inelastic response or the higher-order response of a structure. Several predictors that target inter-story drift angles have been proposed using the results of a nonlinear static pushover (NSP), which in the last decade became a practical engineering tool for estimating the inelastic response of a multi-story frame.

The Limit Strength Calculation method (LSC) was introduced in the Enforcement Order in Japan in 2000 as a seismic design rule for ordinary building structures. Considering the inelastic first-mode response, inter-story drifts are evaluated (Kuramoto et al. 2001). However, the higher-order-mode responses are neglected, and accordingly, the response at upper stories of a long-period building are not generally estimated accurately (Mori, 2004).

Luco (2002) and Cornell proposed an intensity measure using the first two elastic modes and the square-root-of-sum-of-squares (SRSS) rule of modal combination, and also taking into account a first-mode inelastic spectral displacement. This intensity measure achieved a marked improvement over simply using the response of an elastic oscillator. However, as a predictor it does not capture well the effects of P-Delta in lower stories and the corresponding "isolation" effect in upper stories.

This paper presents a new predictor of seismic demand that is based on Luco's intensity measure but considers a post-elastic mode shape. The accuracy of the predictor is demonstrated for several steel moment-resisting frame (SMRF) buildings.

2. BUILDING MODELS

In this investigation of the accuracy of predictors, two-dimensional fishbone models of one low- and two mid-rise SMRF buildings are considered; the four- and nine-story buildings designed according to Japanese practice are denoted as JP4 and JP9, respectively, and the nine-story building designed according to U.S. practice is denoted as SAC9. The first- and second-mode periods, T_1 and T_2, and Rayleigh damping ratios, h_1 and h_2, of each building model are listed in Table 1.

The fishbone model of a frame condenses all of the columns in a story into a single column, and all of the beams in a floor into a singe rotational beam spring. Accordingly, the number of degrees of freedom can be reduced significantly while keeping almost the same accuracy as nonlinear dynamic analysis (NDA) of a full-frame model (Nakashima et al., 2002; Luco et al., 2003). The key assumption is that the rotations at all of the beam-column connections in a floor are identical. The details of this condensation are explained in (Nakashima et al., 2002), but a few important characteristics of the fishbone models considered in this paper are listed here:

(1) The single beam spring for each floor is trilinear, while bilinear plastic hinging at the column ends and splices is modeled for all but JP9 (explained below). The ratios of the strain-hardening slope to the elastic slope for the beams, α_B, and for the columns, α_C, of each building model are listed in Table 1. Column P-M interactions due to tributary gravity loads, but not due to varying axial forces caused by overturning, are taken into account.
(2) Global (but not member) P-Δ effects are accounted for, with all applicable gravity loads placed on the fishbone column.

Other details specific to each of the three buildings are provided in the subsections below.

2.1 JP9 Building

JP9 is a 9-story SMRF building designed directly as a fishbone models as follows:

- The height of each story is 4.0m, and the mass is distributed equally among the floors.
- The story-shear force distribution coefficient, A_i, is given by

$$A_i = 1/\sqrt{\alpha_i} \tag{1}$$

  where α_i is the ratio of the mass above the i-th story to the total mass of the building.
- Assuming that the inflection point of each column is located at the mid-height of each story, all the beams are designed to yield simultaneously when the normalized base shear, C_0, is equal to 0.2. The stiffness is designed so that the inter-story drift angle at this point is 1/200 of the height of each story.
- When $C_0 = 0.3$, the moments at all of the beams and at the column base of the first story are equal to their maximum strengths.
- The hinging at the first-story column base is modeled as rigid-perfectly-plastic, while the rest of the fishbone column is assumed to be elastic.

Table 1: Structural characteristics of fishbone models

Building Model	T_1 (sec)	T_2 (sec)	h_1 (%)	h_2 (%)	α_B (%)	α_C (%)
JP9	1.50	0.56	2.0	2.0	0	0 (base column of the 1st floor)
SAC9	2.24	0.84	2.0	1.1	3	3
JP4	0.79	0.28	2.0	2.0	2	1

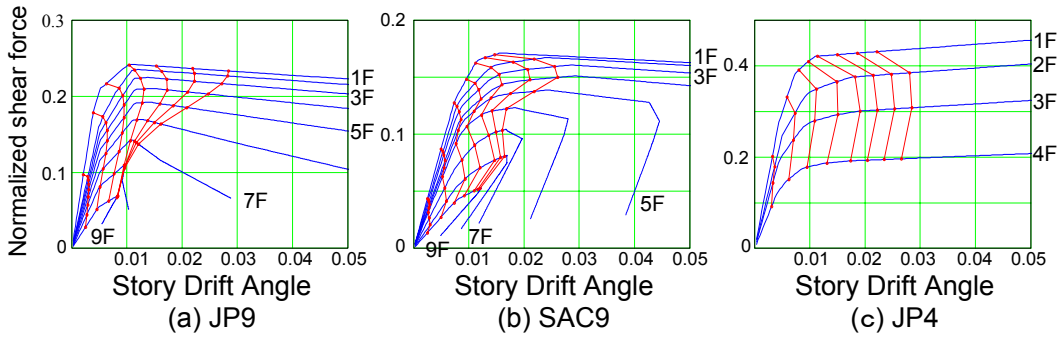

Figure 1: Nonlinear static pushover curves

- The ratio of the elastic stiffness of a beam spring to that of the column is unity.

2.2 SAC9 Building

SAC9 is a 9-story perimeter SMRF building designed for Los Angeles conditions by consulting structural engineers as part of Phase II of the SAC Steel Project (FEMA 355C, 2000). Only one of the 5-bay perimeter MRF's is modeled, although gravity loads from half of the building are considered since they contribute to the P-Δ effect. The interior frames are assumed to resist gravity loads only.

2.3 JP4 Building

JP4 is a 4-bay and 4-story SMRF building designed by a structural engineer according to Japanese practices (The BRI and Kozai Club, 1995). Unlike SAC9, all of the perimeter and interior frames, and all of the beam-column connections of JP4 are moment-resisting. Only one of these frames is modeled, taking into account its tributary gravity loads.

The NSP curves for all of the models using lateral load patterns proportional to the A_i-distribution given in the Enforcement Order in Japan are illustrated in Figs.1(a)JP9, (b)SAC9, and (c)JP4. More detailed descriptions of the SAC9 and JP4 buildings can be found in (Luco et al., 2003).

3. EARTHQUAKE GROUND MOTION RECORDS

So-called "nearby-field" earthquake records were selected from the PEER Strong Motion Database (http://peer.berkeley.edu/smcat) according to the following criteria: (i) closest distance to the rupture surface less than 16km, (ii) earthquake moment magnitude greater than or equal to 6.0, (iii) recorded on "stiff soil" or "very dense soil and soft rock" (e.g., FEMA 273 (1997) site classes D or C, respectively), and (iv) high-pass-filter corner frequency less than or equal to 0.25 hertz. Only the strike-normal components are used. Of the resulting 73 nearby-field ground motions, 70 were recorded in California, and the other 3 were recorded in Erzican (Turkey), Tabas (Iran), and Kobe. A detailed list of the earthquakes can be found in (Luco, 2002). Despite their proximity to the earthquake source, it is important to note that not all of the nearby-field earthquake records are "pulse-like" (i.e., not all exhibit a low frequency, large amplitude pulse in the velocity time history). In fact, less than half of the nearby-field ground motions are recorded in the region where forward rupture-directivity effects are anticipated, and even those are not all pulse-like (Luco, 2002).

4. EXISTING PREDICTORS

Among existing predictors, the LCM predictor and Luco's intensity measure (considered as a predictor) are briefly reviewed in this section and their accuracy is investigated.

4.1 Limit Capacity method

In the LCM method the inter-story drift angles of a building are evaluated as follows (Kuramoto et al., 2001):

(1) Determine the step-by-step "shear force - story drift relationship" for each story by a NSP with lateral load pattern proportional to the A_i-distribution determined in the Enforcement Order in Japan.

(2) Determine the step-by-step S_A-S_D relationship according to the Capacity Spectrum approach (Freeman, 1978):

$$S_{Aj} = \frac{\sum_{i=1}^{n} m_i \cdot \delta_{ij}^2}{(\sum_{i=1}^{n} m_i \cdot \delta_{ij})^2} Q_{Bj} \tag{2}$$

$$S_{Dj} = \frac{\sum_{i=1}^{n} m_i \cdot \delta_{ij}^2}{\sum_{i=1}^{n} m_i \cdot \delta_{ij}} \tag{3}$$

in which Q_{Bj} and δ_{ij} are the base shear and the drift of the i-th story at the j-th step of the NSP, respectively, m_i is the mass at the i-th floor, and n is the number of stories.

(3) Simplify this Capacity Spectrum curve to be trilinear.

(4) Determine the backbone curve (Q-Δ relation) of the equivalent nonlinear SDOF system by setting $Q = S_A \cdot M_e$ and $\Delta = S_D$, where M_e is the equivalent mass when the building is in its elastic range.

(5) Perform NDA to evaluate the maximum drift, Δ_{max}, of the equivalent SDOF system with the backbone curve determined in Step (4) and M_e.

(6) Find the step number, n_p, of the NSP at which the drift $S_D = \Delta_{max}$.

(7) Assume that the shear forces and story displacements at the n_p-th step of the NSP from Step (1) are those of the multi-story frame subjected to the ground motion of interest. This is the predictor of inter-story drift angle for the k-th story, $\hat{\theta}_k^{LCM}$.

4.2 Luco's Predictor

Luco and Cornell proposed an intensity measure using the first two elastic modes and the SRSS rule of modal combination, multiplied by the ratio of a first-mode inelastic spectral displacement to the first-mode elastic spectral displacement (Luco and Cornell, 2003):

$$\hat{\theta}_k^{Luco} = PF_{1,k} \cdot S_D^I(T_1, h_1, \delta_y, \alpha) \sqrt{1 + \frac{\{PF_{2,k} \cdot S_D(T_2, h_2)\}^2}{\{PF_{1,k} \cdot S_D(T_1, h_1)\}^2}} \tag{4}$$

in which $S_D(T_1, h_1)$ is the elastic spectral displacement of a SDOF system with natural period T_1 and damping factor h_1, $S_D^I(T_1, h_1, \delta_y, \alpha)$ is the inelastic spectral displacement of a bilinear SDOF system with yield displacement δ_y and strain hardening ratio α (in addition to T_1 and h_1), and $PF_{j,k}$ is the participation factor of the j-th mode (for the k-th story) defined by

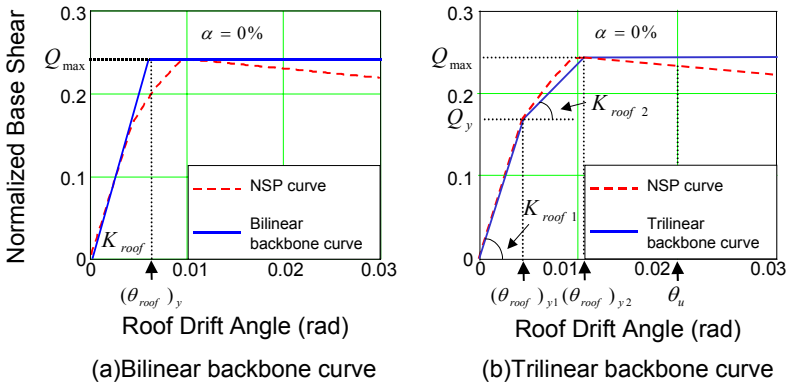

Figure 2: NSP curve for the JP9 model, and the backbone curves fit to it

$$PF_{j,k} = \Gamma_j \frac{\phi_{j,k} - \phi_{j,k-1}}{H_k} \tag{5}$$

where $\phi_{j,k}$ is the element of the j-th mode vector that corresponds to the k-th floor, H_k is the height of the k-th story, and

$$\Gamma_j = \frac{\sum_{i=1}^{n} \phi_{j,i} \cdot m_i}{\sum_{i=1}^{n} \phi_{j,i}^2 \cdot m_i} \tag{6}$$

The backbone curve of the inelastic SDOF system (i.e., δ_y and α) is based on the roof drift versus base shear curve from a NSP of the structure. If the NSP curve is either nearly plastic or degrading, the curve is idealized as elastic-perfectly-plastic (i.e., $\alpha = 0$) to determine δ_y. The elastic slope of the idealization follows the elastic points of the NSP curve, whereas the perfectly-plastic slope passes through the peak base shear (up to a roof drift angle of 0.10 rad). The intersection of the two slopes provides an estimate of the roof drift angle at yield, denoted $(\theta_{roof})_y$ (see Fig.2(a)), which is translated into δ_y according to Eq.(7)

$$\delta_y = (\theta_{roof})_y \cdot \sum_{k=1}^{n} H_k / (\Gamma_1 \cdot \phi_{1,n}) \tag{7}$$

4.3 Accuracy of Existing Predictors

The accuracy of a predictor is expressed by (i) its bias, a, defined by the "median" (strictly the geometric mean) of $\theta/\hat{\theta}$, which is the ratio of the demand computed via NDA of the model structure to the corresponding value of the predictor, and (ii) its "dispersion," σ, defined by the standard deviation of the natural logarithms of $\theta/\hat{\theta}$. The bias, a, and the precision, σ, are equivalently obtained by performing a one-parameter log-log linear least-squares regression of θ on $\hat{\theta}$. The regression model is expressed by

$$\ln(\theta) = \ln(a) + \ln(\hat{\theta}) + \ln(\varepsilon) \tag{8}$$

in which ε is the random error in θ given $\hat{\theta}$ with (by definition) median 1 and dispersion σ. The predictor of θ_{max} (the maximum peak story drift angle over all stories), as well as the predictor of θ_k (the peak story drift angle for story k), are compared with the quantities numerically evaluated by NDA in the following.

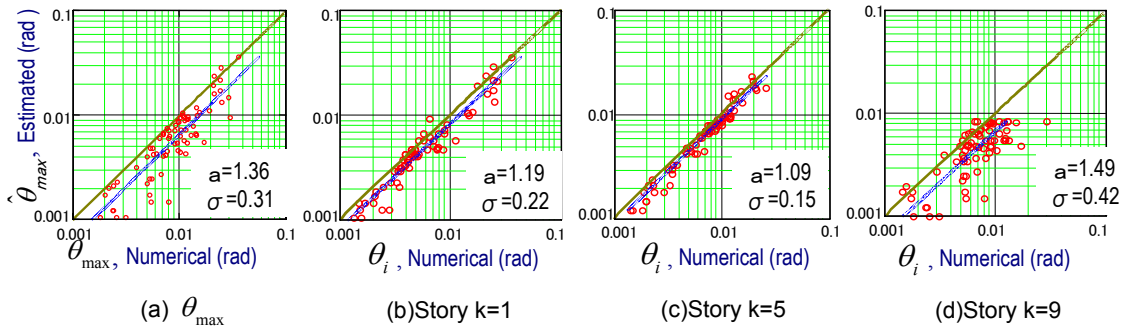

Figure 3: Regressions of θ on $\hat{\theta}^{LCM}$ for the fishbone model of JP9

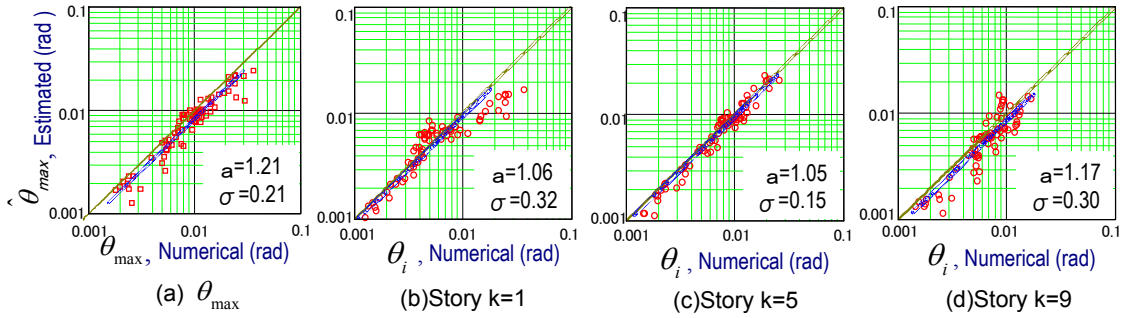

Figure 4: Regressions of θ on $\hat{\theta}^{Luco}$ for the fishbone model of JP9

Figs.3 (a)-(d) illustrate the regressions of (a) θ_{max} and θ_k (k =(b) 1, (c) 5, (d) 9) on the predictor $\hat{\theta}^{\rm LCM}_{max}$ and $\hat{\theta}^{\rm LCM}_k$, respectively, for the JP9 building subjected to the nearby-field earthquake records. A thick solid line in each figure shows the regression relation.

The bias and the dispersion of the LCM predictor at the first and the fifth stories are relatively small, although the response tends to be slightly underestimated. However, the bias and the dispersion is very large (a=1.49 and σ=0.42) at the ninth story. In the LCM method, only the first-mode response is considered, and the inter-story drifts from the NSP at the step corresponding to the maximum drift of the inelastic SDOF system are directly used as the peak response to a ground motion. For buildings in which the NSP drifts at some stories stop increasing, or even decrease, with increasing lateral loads, there will be an upper limit on the drifts predicted by the LCM in those stories (e.g., see Fig.1(a)).

Figs.4 (a)-(d) illustrate the regressions of (a) θ_{max} and θ_k (k =(b) 1, (c) 5, (d) 9) on the predictor $\hat{\theta}^{\rm Luco}_{max}$ and $\hat{\theta}^{\rm Luco}_k$, respectively, also for the JP9 building. The bias and the dispersion of $\hat{\theta}^{\rm Luco}_{max}$ and $\hat{\theta}^{\rm Luco}_k$ are generally small. However, some systematic deviations from the regression line can be observed at the first and ninth stories. At the first story, the predictor tends to underestimate the larger responses; in contrast, it tends to overestimate the responses near yielding ($\theta_1 \approx 0.005$), possibly because of the simple approximation of the backbone curve of the SDOF system as bilinear (see Fig.2(a)). At the ninth story, $\hat{\theta}^{\rm Luco}_k$ tends to overestimate the larger responses, while it tends to underestimate the smaller responses, possibly because of the neglect of the modal responses higher than the second.

Figs.5 (a) and (b) illustrate, for two different ground motions, θ_k and $\hat{\theta}^{\rm Luco}_k$ for the JP9 building, plotted story-wise. It can be observed in these figures that the predictor does not capture the large responses at lower stories. Only the elastic first- and second-mode shapes are considered in Luco's

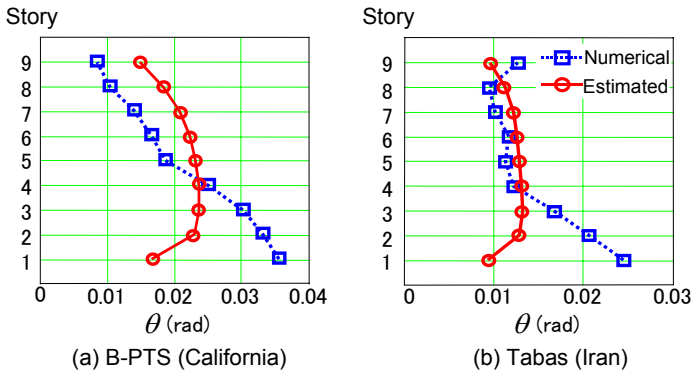

Figure 5: Examples of Luco's predictors

predictor, but the large responses at the lower stories after yielding are not predicted well using only the elastic mode shapes. Accordingly, it is necessary to consider a post-elastic mode shape.

Since each mode shape changes as plastic hinges are formulated, a post-elastic mode shape must consider the ductility level. One idea is to track the formulation of plastic hinges in the NSP and perform an eigen value analysis for each stage. However, this is complicated. Another possibility is investigated in the next section.

5. PREDICTOR CONSIDERING POST-ELASTIC MODE SHAPE

Based on the observations in the previous section, an improved predictor based on Luco's intensity measure is proposed in this section by considering (i) a post-elastic mode vector dependent upon the ductility level, (ii) a more appropriate backbone curve for the equivalent SDOF system, and (iii) higher-order modal response. Assuming that a post-elastic mode vector, $\boldsymbol{\phi}_1^I$, can be approximated by the distribution of story drifts from a NSP, it is determined for each ground motion by taking the following steps (see Fig.6).

(1) Perform a NSP with the lateral load pattern proportional to the A_i-distribution given in the Enforcement Order in Japan, which takes into account the effects of higher-order modal response,

(2) Obtain the normalized story shear - story drift curve (e.g., see Fig.1), as well as the normalized base shear, C_0, - roof drift, θ_{roof}, curve,

(3) Approximate the C_0-θ_{roof} curve as trilinear with final strain-hardening ratio $\alpha = 0$ (e.g., see Fig.2(b)),

(4) Determine the backbone curve of an equivalent SDOF system using Eq.(7). The second stiffness of the backbone curve, k_2, is determined by

$$k_2 = k_1 \cdot \frac{(K_{roof})_2}{(K_{roof})_1} \tag{9}$$

in which k_1 is the elastic stiffness of the SDOF system, and $(K_{roof})_1$ and $(K_{roof})_2$ are the elastic and second stiffnesses of the C_0-θ_{roof} curve approximated in Step (3),

(5) Perform NDA to evaluate the maximum drift, Δ_{max}, of the equivalent SDOF system,

(6) By the inverse of Step (4), find the roof drift of the building on the C_0-θ_{roof} curve corresponding to Δ_{max},

(7) Determine the step number, n_p, of the NSP for the roof drift angle found in Step (6),

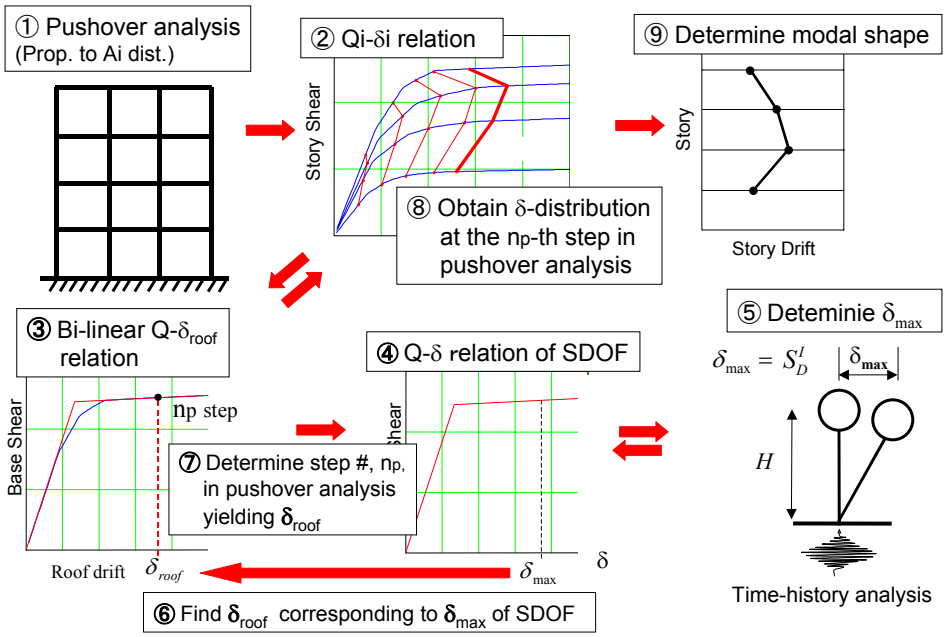

Figure 6: Flow for determining the 1st inelastic mode vector $\phi^I_{1,k}$

(8) Find the story drift at the n_p-th step of the NSP,
(9) Use the distribution of story drifts obtained in Step (8) as the post-elastic first-mode shape.

Considering up to the third mode, the proposed predictor of the inter-story drift angle for the k-th story is evaluated by,

$$\hat{\theta}_k^{new} = \sqrt{\left\{PF^I_{1,k} \cdot S^I_D\left(T_1, h_1, \delta_y, \alpha\right)\right\}^2 + \{PF_{2,k} \cdot S_D(T_2, h_2)\}^2 + \{PF_{3,k} \cdot S_D(T_3, h_3)\}^2} \qquad (10)$$

where $PF^I_{1,k}$ is evaluated by Eqs.(5) and (6) in which $\phi_{1,k}$ is replaced with the "inelastic first-mode shape" determined above.

It should be noted that the additional work in the above procedure is minimal as NSP is already carried out to determine an equivalent SDOF system for Luco's intensity measure.

6. NUMERICAL EXAMPLE

Figs.7 (a)-(d) illustrate the regressions of (a) θ_{max} and θ_k (k =(b) 1, (c) 5, (d) 9) on the predictor $\hat{\theta}^{\text{new}}_{max}$ and $\hat{\theta}^{\text{new}}_k$ for the JP9 building subjected to the nearby-field earthquake records. The bias of $\hat{\theta}^{\text{new}}_{max}$ becomes closer to unity than that of $\hat{\theta}^{\text{LCM}}_{max}$ and $\hat{\theta}^{\text{Luco}}_{max}$, and the dispersion decreases by two-thirds to a half. At the first story, the underestimation of the large responses and the overestimation of the responses near $\theta_1 \approx 0.005$ are improved with respect to Luco's intensity measure by considering the post-elastic first-mode shape and adopting a trilinear backbone curve for the equivalent SDOF system. The underestimation of the smaller responses at the ninth story is also improved by considering the third-mode response.

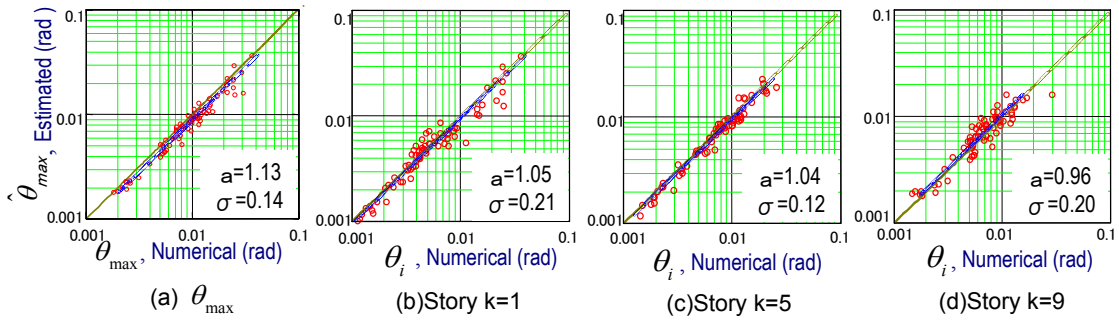

Figure 7: Regressions of θ on $\hat{\theta}^{new}$ for the fishbone model of JP9

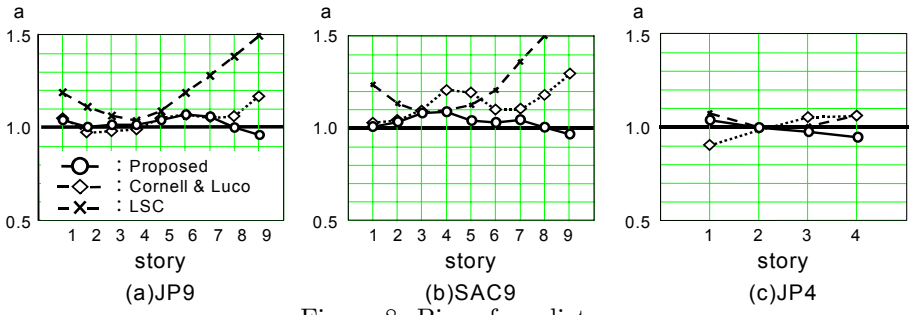

Figure 8: Bias of predictors

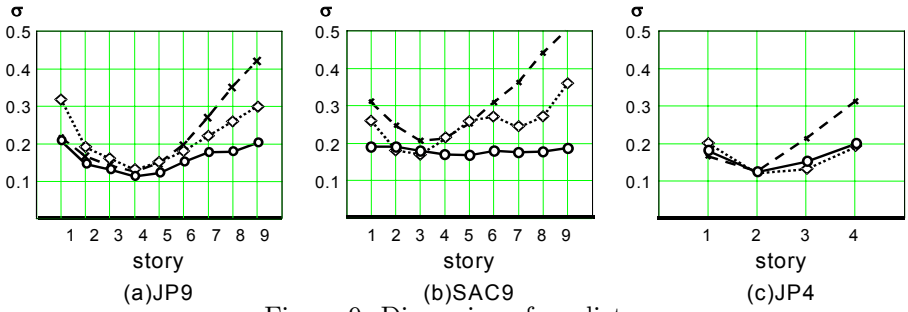

Figure 9: Dispersion of predictors

Figs.8(a)-(c) and 9(a)-(c) summarize the bias and the dispersion, respectively, of the LCM, Luco's and the proposed predictors for the (a)JP9, (b)SAC9, and (c)JP4 buildings subjected to the nearby-field earthquake records. The bias of the proposed method is fairly stable and within the range of 0.9 - 1.1 for all of the buildings. On the contrary, the bias of LCM is fairly large ($a > 1.3$) at the upper stories of the nine-story buildings because of the lack of consideration of the higher-order modes. For the JP9 building, the bias of Luco's intensity measure is comparable with that of the proposed method, except for at the 9th story; however, for the SAC9 building, relatively large bias is observed at the middle and upper stories ($a > 1.2$). For the JP4 building, the biases of all three predictors are comparable.

It can be observed in Figs.9(a) -(c) that the dispersion of the proposed method is also fairly stable and less than about 0.20 at every story of all of the buildings. On the contrary, the dispersion of the LCM predictor and Luco's intensity measure are larger than 0.25 at many stories and even larger than 0.35 at some stories for the 9-story buildings. The dispersion of the LCM predictor at the fourth story of the JP4 is larger than that of the other predictors despite the small contribution of higher-order modal responses.

7. CONCLUSIONS

Predictors of seismic inter-story drift angles for practical use in structural performance assessment and design are investigated in this paper. In addition to the inelastic first-mode spectral displacement considered in Luco's intensity measure based otherwise on SRSS modal combination, it is proposed to consider (i) a post-elastic first-mode shape approximated by the distribution of story drifts from a NSP at the step corresponding to the maximum drift of the equivalent inelastic SDOF system, (ii) a trilinear backbone curve for the SDOF system, and (iii) the third-mode response for long-period buildings. Numerical examples demonstrate that the proposed predictor is less biased and results in less dispersion than Luco's intensity measure and the Limit Strength Calculation method. Further evaluation of the proposed predictor for additional earthquake records and structures of different fundamental periods, heights, and configurations is being conducted in order to find any limitations.

ACKNOWLEDGEMENTS

The authors gratefully acknowledge the financial support of the U.S.-Japan Cooperative Research in Urban Earthquake Disaster Mitigation Project (NSF 98-36) under grant number CMS-9821096, and the Grant-in-Aid for Scientific Research (B) (No.11209204) from the Ministry of Education, Science, Sports, and Culture and Japan Society for the Promotion of Science.

REFERENCES

The BRI and Kozai Club. (1995), *Evaluation of plastic deformation responses of steel moment frames subjected to earthquake motions*, Report of Committee on Numerical Analysis Procedures 1995.

Freeman, S.A. (1978), "Prediction of Response of Concrete Buildings to Severe Earthquake Motion," *Douglas McHenry Int. Symp. on Concrete and Concrete Structures*, SP-55, ACI, pp.589-605.

FEMA 273. (1997), *NEHRP guidelines for the seismic rehabilitation of buildings*, Federal Emergency Management Agency, Washington, D.C.

FEMA 355C. (2000), *State of the art report on systems performance of steel moment frames subject to earthquake ground shaking*, SAC Joint Venture; Sacramento, California.

Kuramoto, H., Teshigawara, M., Koshika, N., and Isoda, H. (2001), "Conversion of Multi-story Building into Equivalent SDOF System and its Predictability for Earthquake Response." *J. Struct. Constr. Engrg.*, AIJ, No.546, 79-85 (in Japanese).

Luco, N. (2002), *Probabilistic seismic demand analysis, SMRF connection fractures, and near-source effects*, Ph.D. Dissertation; Department of Civil and Environmental Engineering, Stanford University: Stanford, California.

Luco, N. and Cornell, C.A. (2003), "Structure-specific scalar intensity measures for near-source and ordinary earthquake ground motions." Under revision for publication in *Earthquake Spectra*.

Luco, N., Mori, Y., Funahashi, Y., Cornell, C.A., and Nakashima, M. (2003), "Evaluation of predictors of nonlinear seismic demands using "fishbone" models of SMRF buildings." *Earthquake Engrg. & Structural Dynamics*, Vol. 32, No. 14, pp.2267-2288.

Nakashima, M., Ogawa, K., and Inoue, K. (2002), "Generic frame model for simulation of earthquake responses of steel moment frames." *Earthquake Engrg. and Structural Dynamics*, Vol.31(3), 671-692.